Anorthosite and associated gabbronorite plutons of Barabar hills in Chotanagpur granite gneiss complex (CGGC), eastern India: Estimation of parental melt for gabbronorite using equilibrium distribution method (EDM)

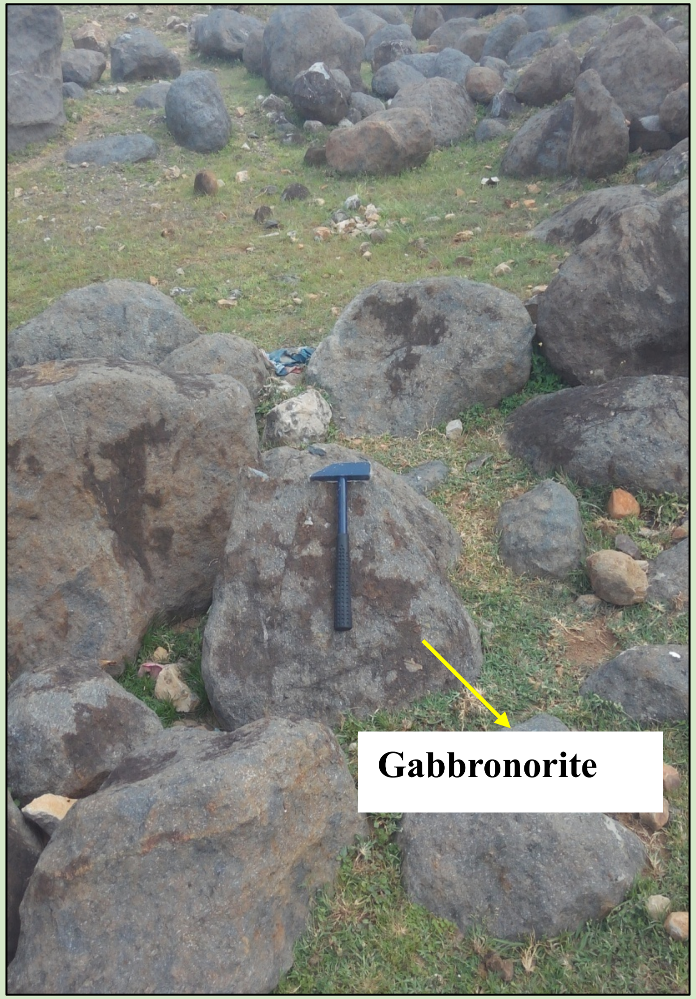

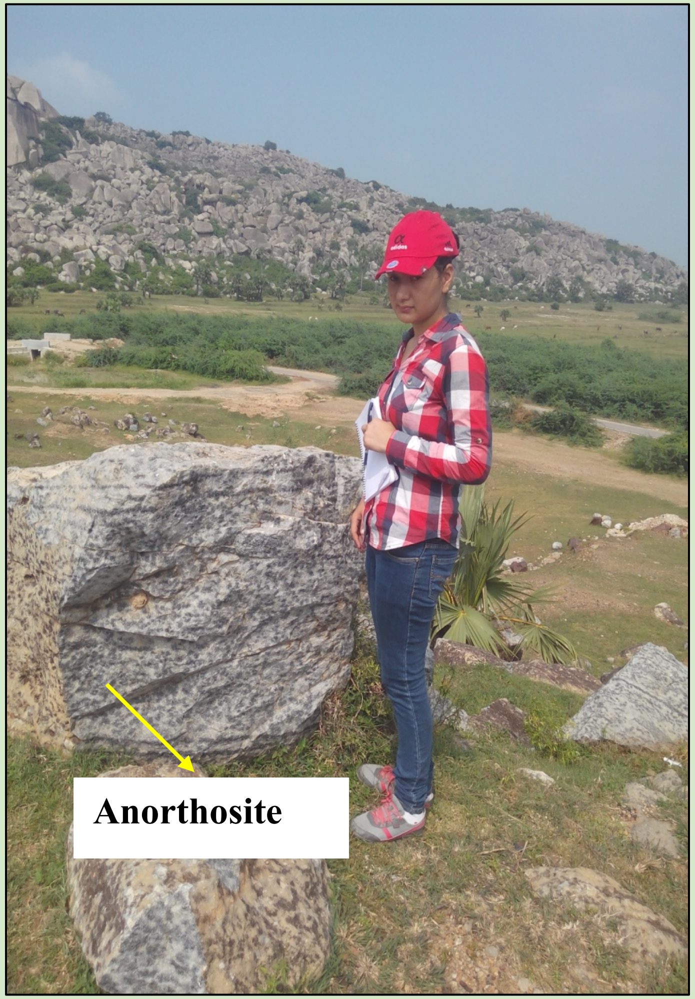

Priyanka Negi[1], Ivan Belousov[2], Leonid V. Danyushevsky[2], Ashima Saikia[1] and Mansoor Ahmad [3]

[1]Department of Geology, University of Delhi, Delhi, India
[2]CODES and Earth Sciences, University of Tasmania, Hobart, TAS 7001, Australia
[3]Geological Survey of India, SU: Jharkhand Ranchi, India.

negipriyanka.du@gmail.com

EGU 2023,24 April 2023

Introduction

- Anorthosite and gabbronorite plutons have been reported from the Barabar hill of the Chotanagpur granite gneiss complex.
- CGGC is considered as the part of CITZ that marks the suture zone between northern and southern Indian blocks.
- Anorthosites of study area occurs as small plutons and they are mainly exist in the association of gabbronorite.
- Understanding the petrogenesis of these rocks will help to gain insights into the link between supercontinent cyclicity witnessed by the Indian land mass and its relation to anorthosite genesis.

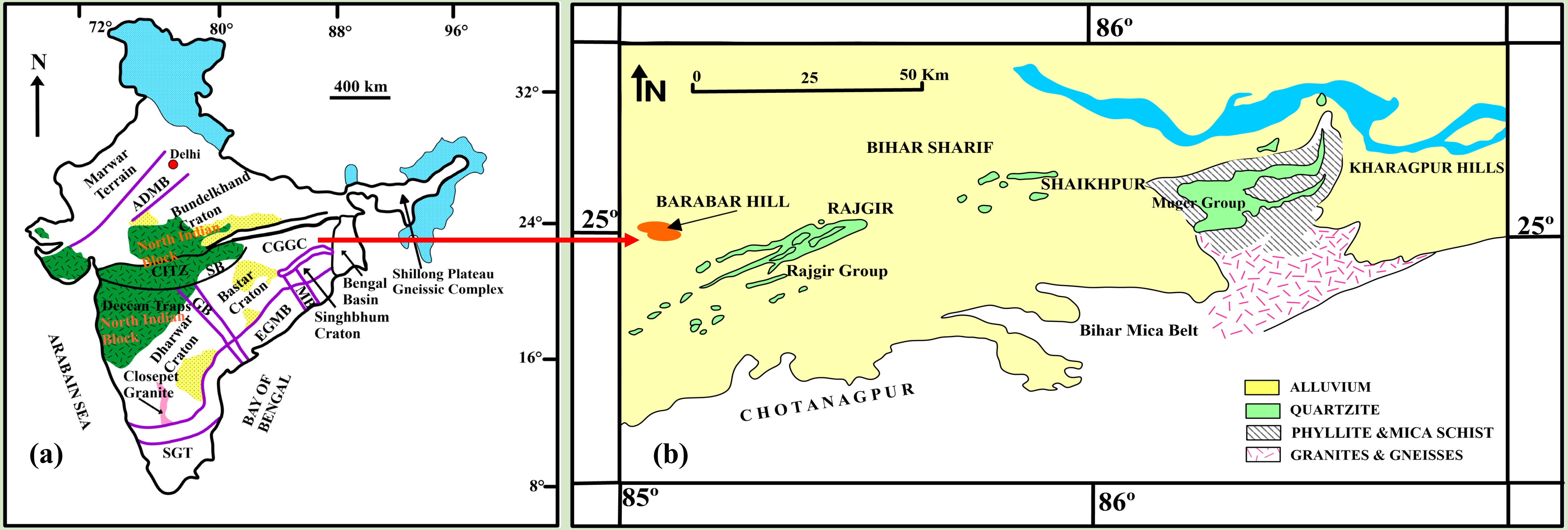

Fig.(a) Simplified geological map of India showing the location of CGGC of eastern India (modified after Pradhan et al., 2009) (b) Map of study area (Courtesy from GSI Report).

Field and petrographic observation

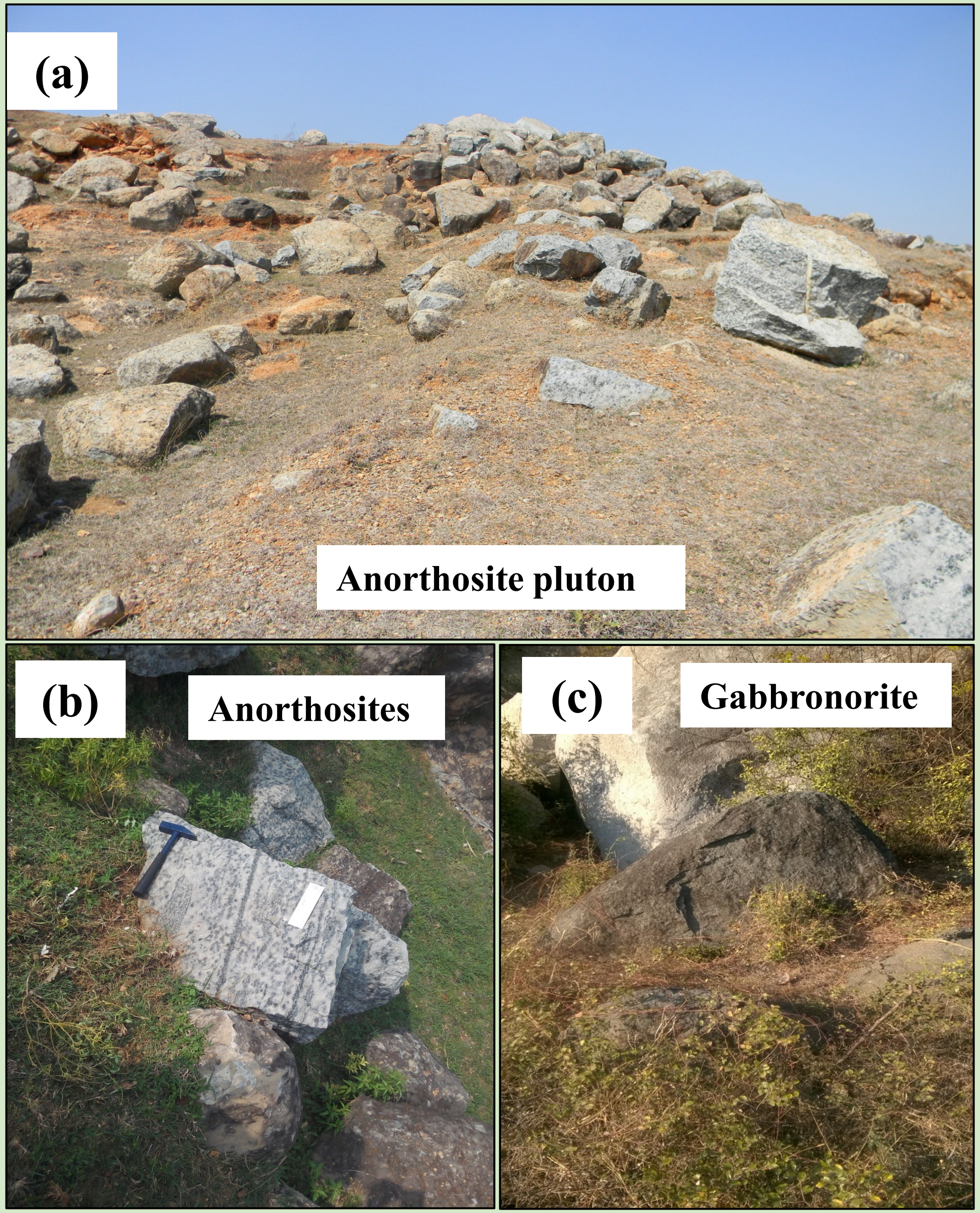

Fig. (a, b) Anorthosites exposures in the study area (C) Outcrop of gabbronorite.

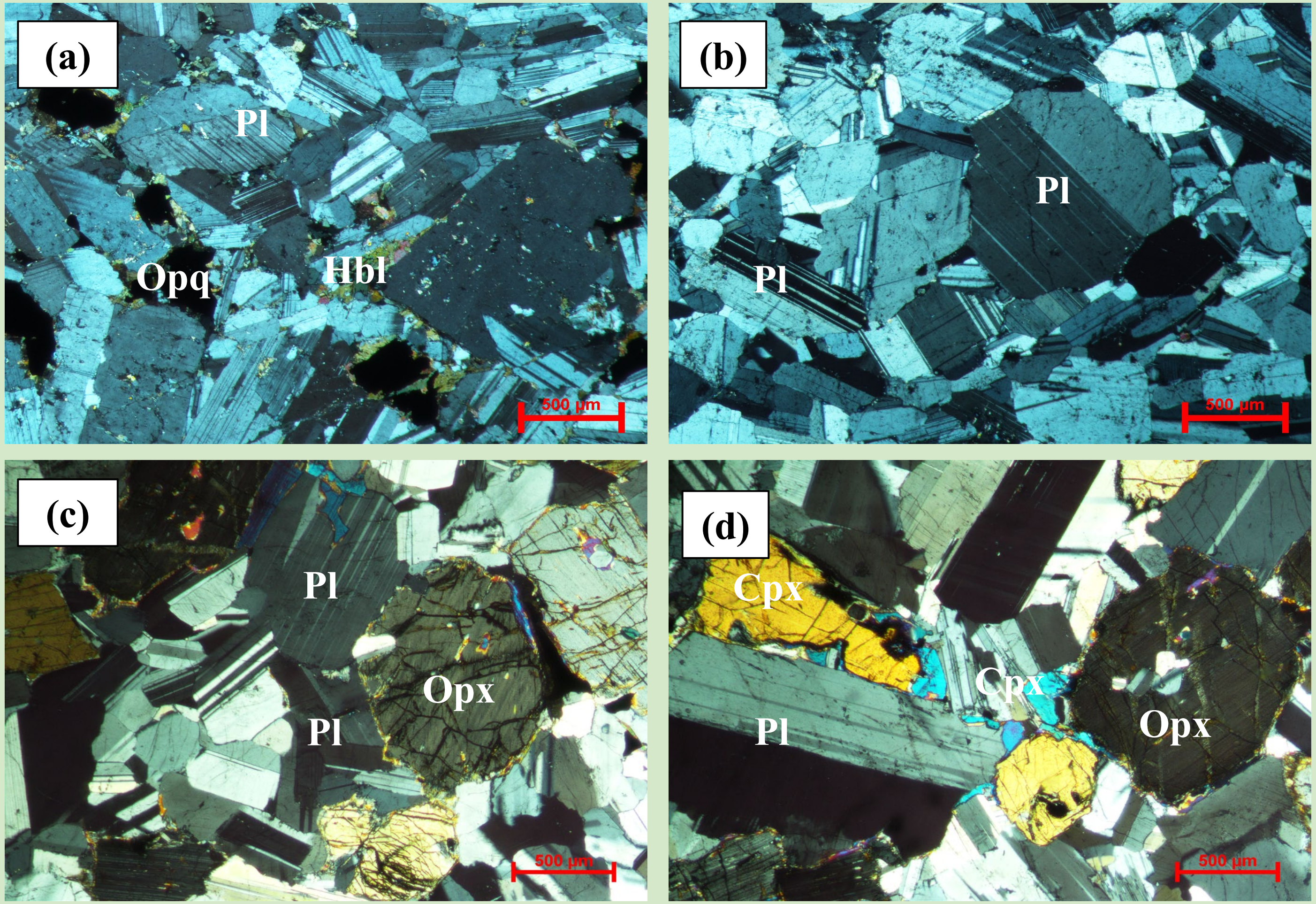

Fig. (a) Photomicrographs of anorthosite showing mineral assemblage of plagioclase (> 95%) + Ca- amphibole (> 5%). (b) anorthosite, mineral assemblage plagioclase (> 98%) (c) Gabbronorite, showing laths of plagioclase associated with orthopyroxene (b) Clinopyroxene as interstitial mineral between plagioclase orthopyroxene , mineral assemblage plagioclase (> 55 %) + Opx (>40 %) + Cpx (< 10%).

Mineral chemical observation of anorthosite and gabbronorite

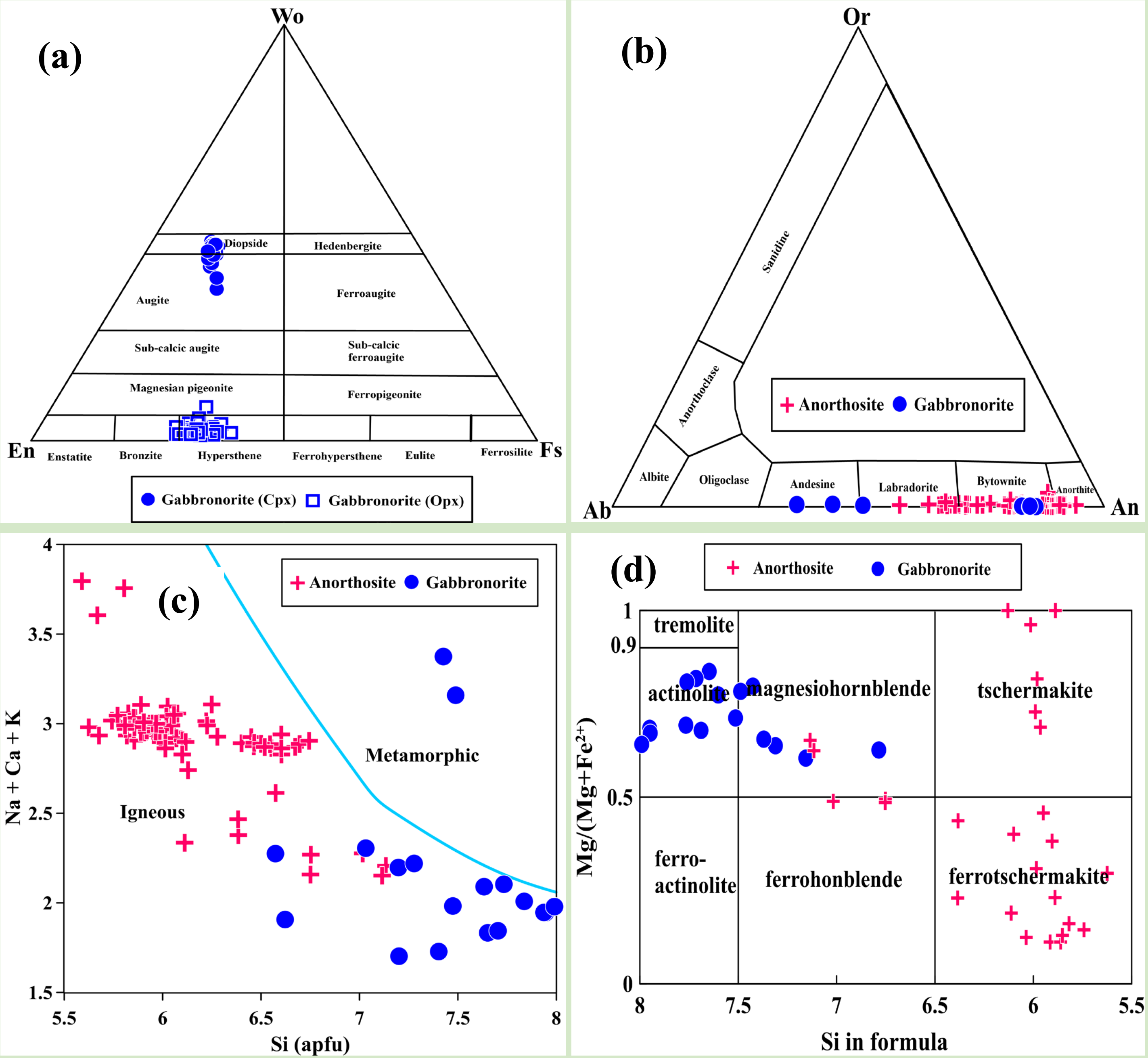

Fig. (a) A triangular plot showing the composition of pyroxene in terms of end-members from the gabbronorite of Barabar hill, CGGC. (modified after Morimoto et al., 1988). (b) Plagioclase composition of the rocks on the Or-Ab-An triangle diagram showing anorthite contains anorthosite, gabbronorite. (modified after Deer et al.1979).

Fig (c) The plot of Si versus Na + Ca + K to discriminate igneous and metamorphic amphiboles (Sial et al., 1998). (d) Amphiboles from Anorthosite, Gabbronorite (after Hawthorne et al., 2012). Nomenclature of amphiboles from the anorthosite and associated gabbronorite from the Barabar hill (after Leake et al., 1997).

Clinopyroxene thermobarometry

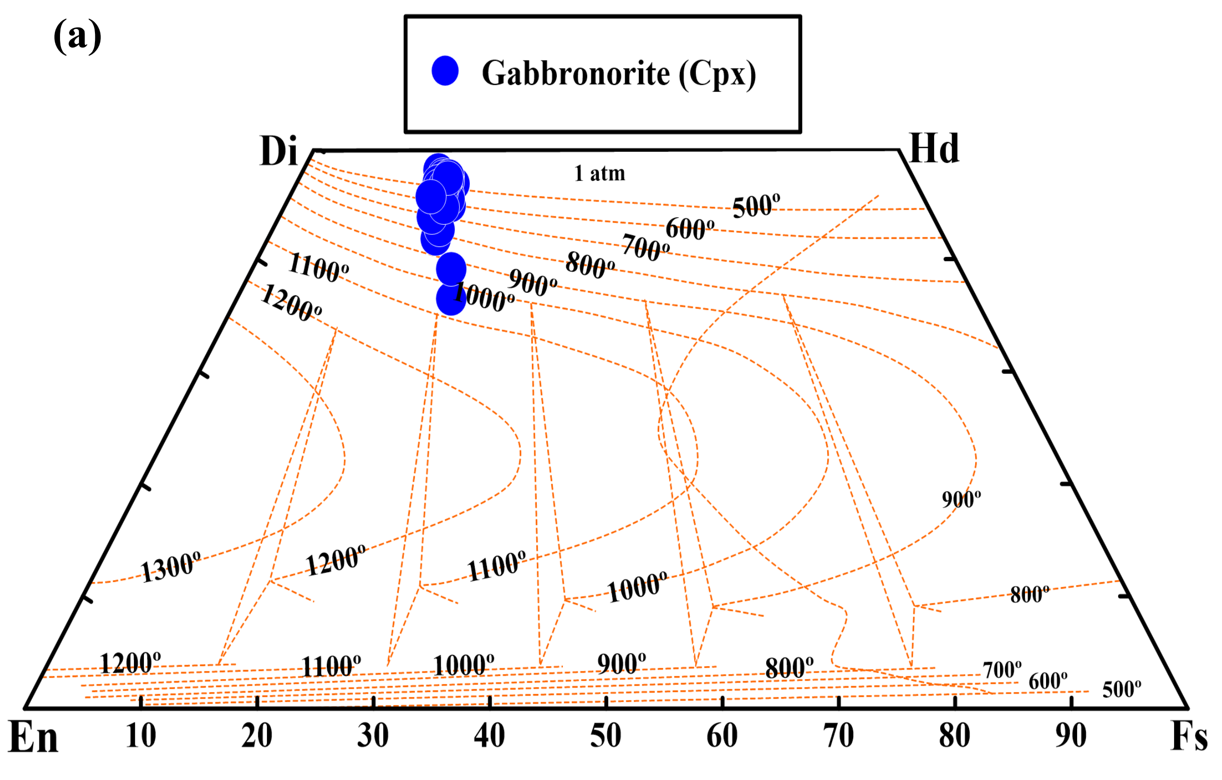

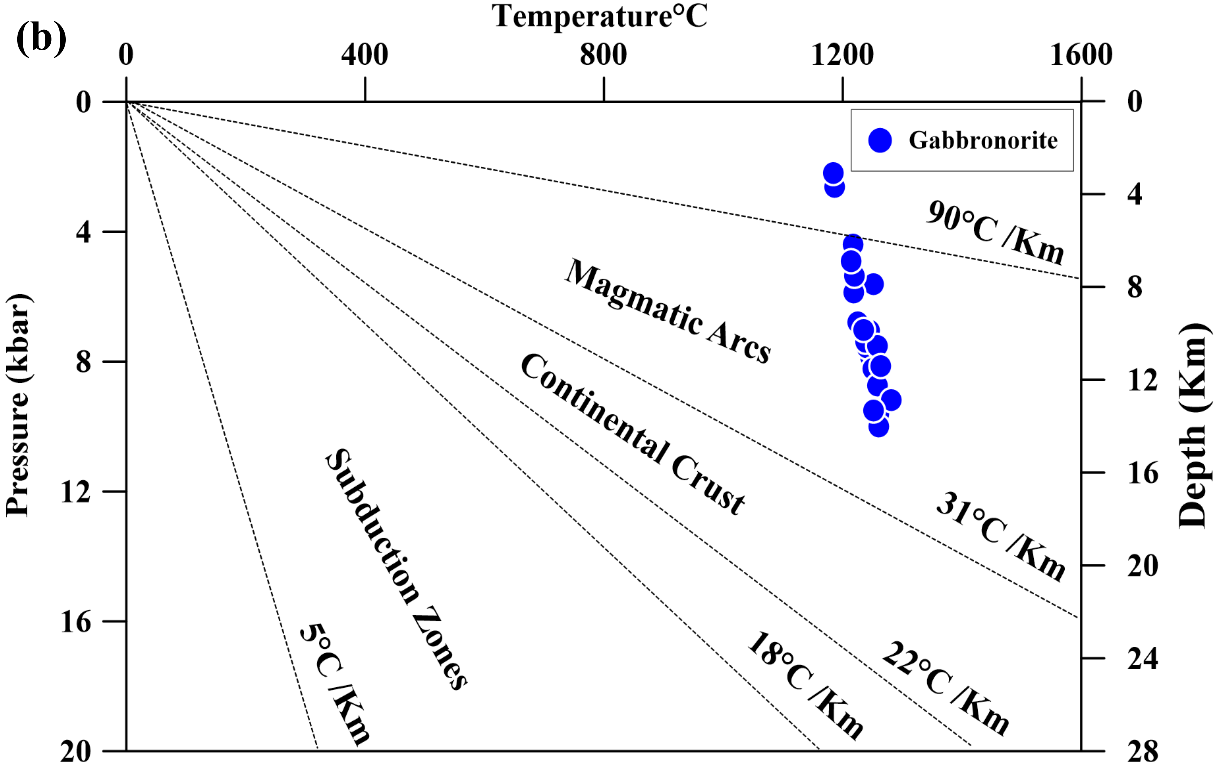

Fig. (a) Pyroxene quadrilateral diagrams (Morimoto et al. 1988) with temperature contours for 5 kbar pressure, using the graphical thermometer of Lindsley (1983). Data are plotted in this diagram, the temperatures of Cpx are 1000−700 °C. Lower temperatures of diopside (< 700 °C) may be due to late-stage re-equilibration during cooling.

(b) Estimated temperature (°C), pressure (kbar) and depth (km) of gabbronorite of Barabar hill calculated based on clinopyroxene only thermo-barometer of Putirka (2008b). Simple linear temperature-depth trends for subduction, continental crust and magmatic arc environments are from Spear (1993).

Geochemical signature of anorthosite

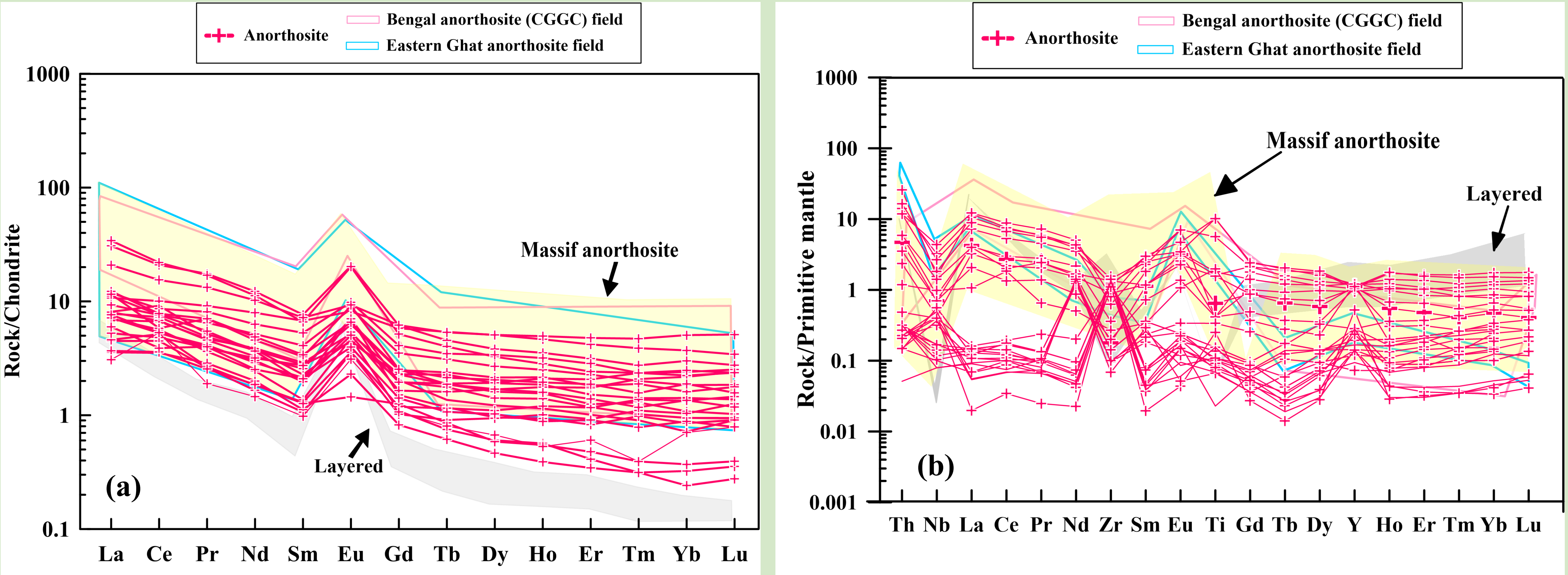

Fig. Multiple element diagrams for anorthosite from Barabar hills compared with the Bengal anorthosites and Anorthosites from Eastern Ghat, India (a) Chondrite-normalized rare earth element trends. (b) Primitive mantle normalized incompatible trace element trends. (Normalization value are after Sun and McDonough,1989 and massif and layered anorthosite fields in the background are from Piaia et al., 2017)

Geochemical signatures of gabbronorite

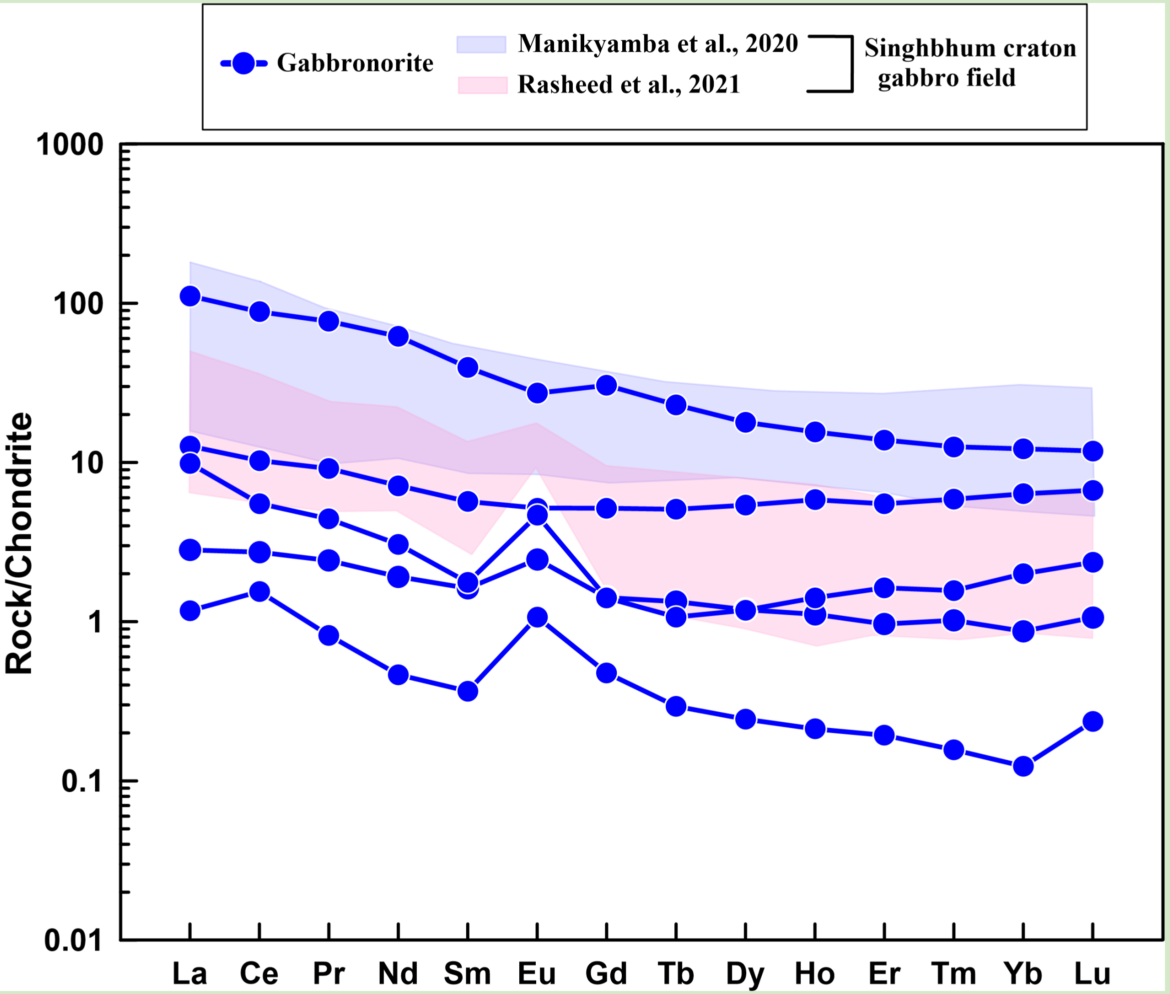

Fig. Chondrite normalized REE diagram of gabbronorite. Plotted for comparison are data of gabbros reported from Singhbhum craton found in association with anorthosites.

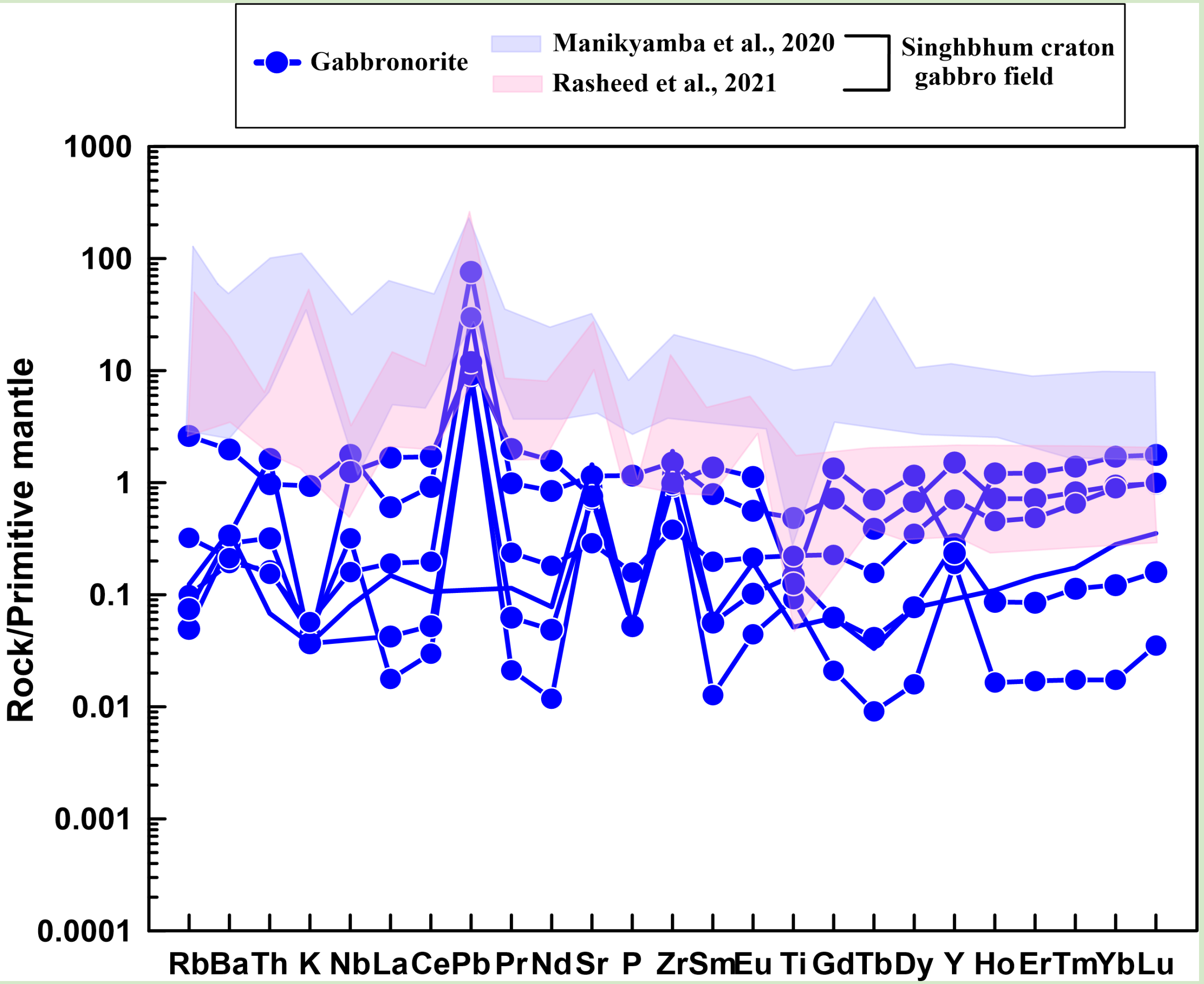

Fig. Primitive mantle normalized spider diagram of gabbronorite. Plotted for comparison are data of gabbros reported from Singhbhum craton found in association with anorthosites.

Parental melt calculations using the equilibrium distribution method

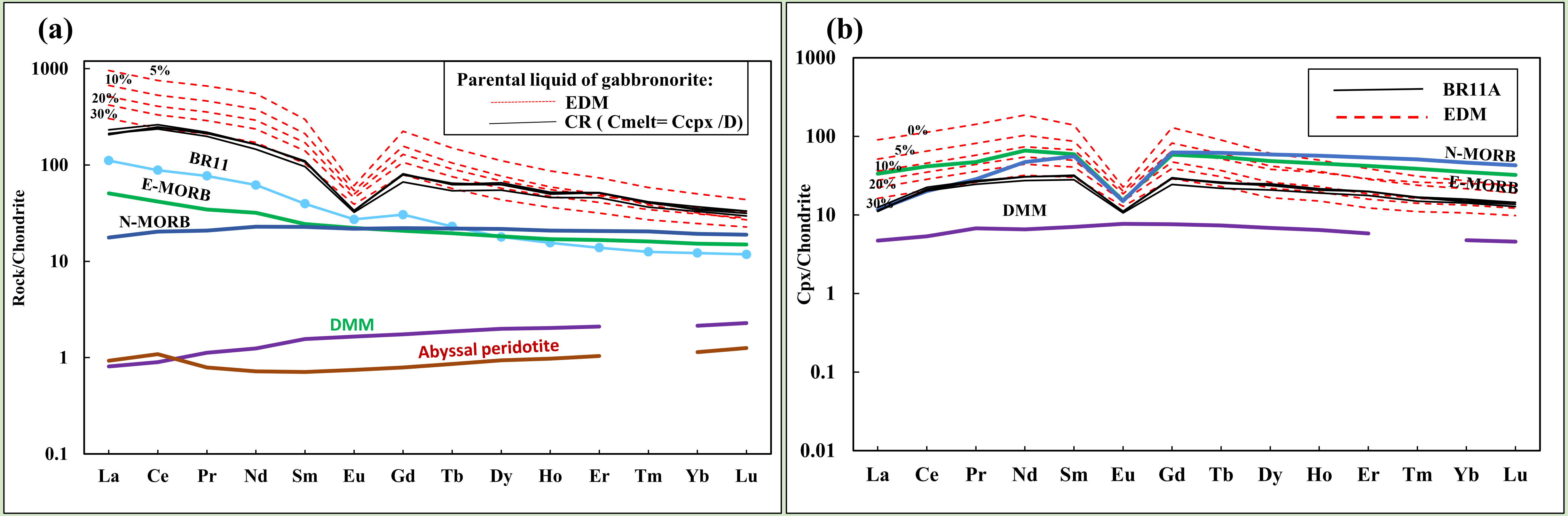

Fig. Chondrite-normalized diagram showing trapped melt and clinopyroxene rare earth element (REE) compositions for samples (a) BR11 and. REE compositions of the clinopyroxenes have been calculated using the equilibrium distribution method (EDM) model of Bédard (1994), assuming a trapped melt fraction (TMF) of 0%, 5%, 10%, 20%, and 30%. Measured clinopyroxene data of the gabbronorite are also shown. The clinopyroxene-melt partition coefficient is taken from Bédard (2014). Clinopyroxene composition of the depleted MORB mantle (DMM) (Workman and Hart 2005), N-MORB (Gale et al. 2013), and average abyssal peridotite (Niu 2004) are also shown for comparison. Normalization values from Sun and McDonough (1989). Whole-rock chondrite-normalized diagram showing trapped melt and REE compositions for samples (b) BR 11 Melt compositions have been calculated using the EDM model of Bédard (1994, 2001), assuming TMF of 0%, 5%, 10%, 20%, and 30%. The whole-rock composition of DMM (Workman and Hart 2005), N-MORB (Gale et al. 2013), and typical abyssal peridotite (Niu 2004) are also shown for comparison.

Model for generation of gabbronorite- anorthosite

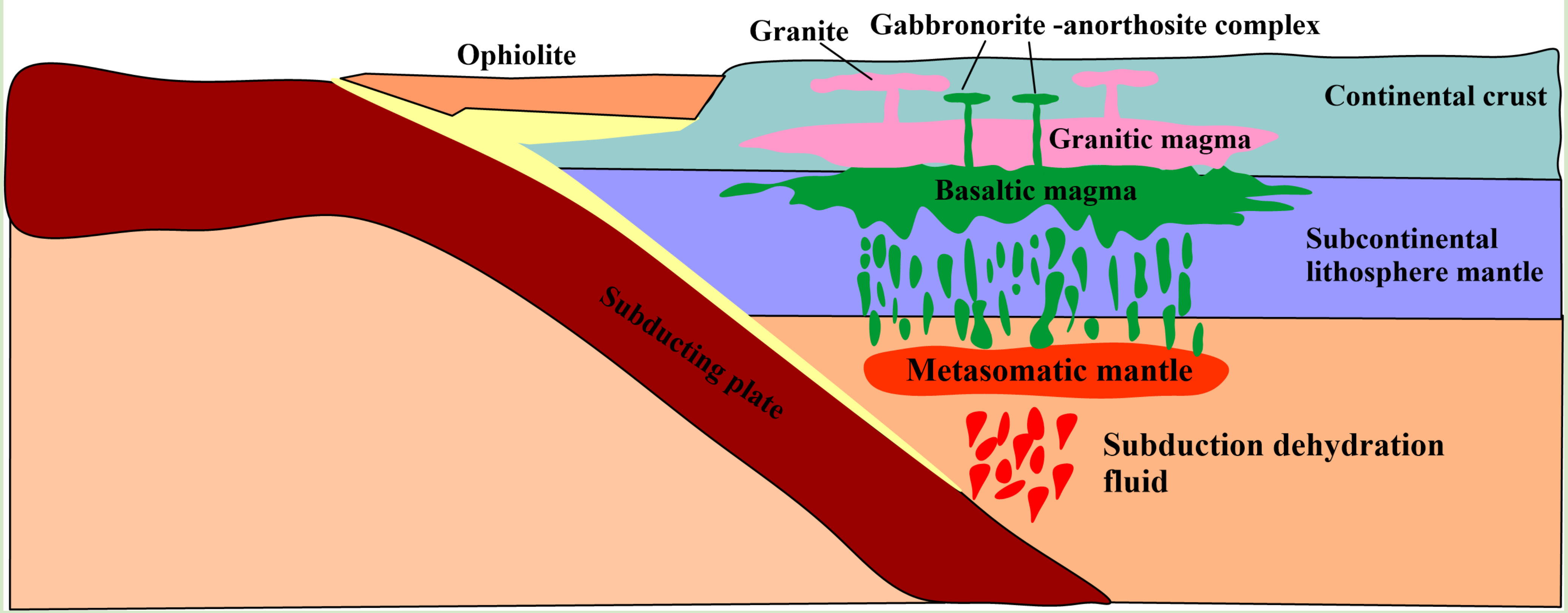

Fig. Cartoon illustrating the plausible formation of the gabbronorite and anorthosite from the Barabar hill , Chotanagpur granite gneiss complex (CGGC)

Conclusions

- **Petrographically the Barabar hill anorthosite consist of plagioclase (> 95%), hornblende (> 5%) and ilmenite occur in the interstics of plagioclase grains as a intercumulus, anorthosite with no mafic content completely consist of plagioclase (> 98%) with no mafic mineral .**

- **For the anorthosites plagioclases have An_{60-100}, amphiboles are tschermakite, ferro-tschermakite, magnesio-hornblende and ferro-hornblende). In gabbronorites plagioclases have An_{30-70} pyroxenes are augite), orthopyroxene are enstatite.**

- **Geochemically anorthosites show enrichment of LREE with flat to depleted trend for HREE [$(La/Yb)_N$=2.79-15.29] and typifies massif type anorthosites and the gabbronorite also show enrichment of LREE but with a flat to slightly enriched trend for HREE.**

- **The EDM modelling of the gabbronorite shows that the whole rock melt curves display near – parallel and increasing trend from Gd to La with negative Eu anomaly. The parental melt calculated by EDM for gabbronorite correspond to liquid at TMF =30%. It is also supported by the composition of parental melt estimated by the concentration method.**

- **Geochemical and mineralogical signatures suggest that the gabbronorite and anorthosite are possibly formed from the same magma source at the depth of 3-10 kbar.**

- **Geochemical signatures suggest origin of anorthosites and associated gabbros in a subduction zone. The area where these rocks occur geologically marks the suturing of the Northern and Southern Indian blocks during the Nuna Supercontinent amalgamation during the Palaeoproterozoic Era.**

References

Barrett TJ, and MacLean WH (1994). Chemostratigraphy and hydrothermal alteration inexploration for VHMS deposits in greenstone and younger volcanic rocks. In D. R. Lentz (Ed.),Alteration and Alteration Processes Associated with Ore-Forming Systems (pp. 433–467).

Bédard JH (1994) A procedure of the calculating equilibrium distribution of trace elements among the minerals of cumulate rocks and the concentration of trace elements in coexisting in liquid. Chemical Geology 118:143–153. https://doi.org/10.1016/0009-2541(94) 90173-2

Bédard JH (2001) Parental magma of Nain plutonic suite anorthosites and mafc cumulates: a trace element modelling approach. Contribution of Mineralogy Petrology 141:747–771. https://doi.org/10.1007/s004100100268.

Bédard JH (2014) Parameterisations of calcic clinopyroxene—melt trace element partition coefcients. Geochemistry Geophysics Geosystems 15(2):303–336. https://doi.org/10.1002/2013GC005112

Deer WA, Howie, RA and Zussman, J. eds., (1997). Rock-forming minerals: single-chain silicates, Volume 2A. Geological Society of London.

Elthon D, (1987) Olivine-liquid partitioning in high-MgO basalt and komatites, In: 18th Lunar and Planetary Science Conference, pp. 258

Gale A, Dalton CA, Langmuir CH, Su Y, Schilling JG (2013) The mean composition of ocean ridge basalts. Geochemistry Geophysics Geosystems 14(2):489–518. https://doi.org/10.1029/2012GC004334

Hawthorne FC, Oberti R, Harlow GE, Maresch WV, Martin, RF, Schumacher, JC, and Welch, MD (2012). Nomenclature of the amphibole supergroup. American Mineralogist, 97(11-12), 2031-2048.

Leake BE, Woolley AR, Arps, CES, Birch WD, Gilbert, MC, Grice, JD, Hawthorne FC, Kato A, Kisch HJ, Krivovichev VG, Linthout K., Laird J, Mandarino JA, Maresch WV, Nickel EH, Rock NMS, Schumacher, J.C., Smith, D.C., Stephenson, N.C.N., Ungaretti, L., Whittaker, E.J.W., and Youzhi, G., 1997, Nomenclature of amphiboles: report of the subcommittee on amphiboles of the International Mineralogical Association, Commission on new minerals and mineral names. Canadian Mineralogist, v. 35, pp. 219−246.

Morimoto N, Fabries J, Ferguson AK, Ginzburg IV, Ross M, Seifert FA, Zussman J, Aoki K, Gottardi G (1988) Nomenclature of pyroxenes. American Mineralogist, 73:1123–1133.

Niu Y (2004) Bulk-rock major and trace element compositions of abyssal peridotites: implications for mantle melting, melt extraction and post-melting processes beneath mid-ocean ridges. Journal of Petrology, 45(12):2423–2458. https://doi.org/10.1093/petrology/egh068.

Piaia P, Oliveira, EP, and Valeriano CM (2017). The 2.58 Ga São José do Jacuipe gabbro-anorthosite stratiform complex, Itabuna-Salvador-Curaçá Orogen, São Francisco Craton, Brazil: Root of the Neoarchaean Caraiba continental arc?. Journal of South American Earth Sciences, 79, 326-341.

Pradhan VR, Meert JG, Pandit MK, Kamenov G, Gregory LC and Malone SJ (2009). India's changing place in global proterozoic reconstructions: A review of geochronologic constraints and paleomagnetic poles from the dharwar, Bundelkhand and marwar cratons. J. Geodyn. 50, 224–242. https://doi.org/10.1016/j.jog.2009.11.008.

Putirka KD (2008). Thermometers and barometers for volcanic systems. In: Putirka K.D., Tepley FJ III (Eds), Minerals, Inclusions and Volcanic Processes. Mineralogical Society of America and Geochemical Society, Reviews in Mineralogy and Geochemistry, v. 69, pp. 61−120.

**Sial AN, Ferreira, VP, Fallick AE, and Cruz MJM (1998). Amphibole rich clots in calc-alkalic granitoids in the Borborema province, northeastern Brazil.
Journal of South American Earth Sciences 11 (5), 457–471.**

Spear FS (1993) Metamorphic Phase Equilibria and Pressure-Temperature-Time Paths. Monograph 1. Mineralogical Society of America: Washington, DC, pp. 799

Sun SS, and McDonough WF (1989) Chemical and isotopic systematic of oceanic basalts: implications for mantle composition and processes. In: Saunders AD, Norry MJ (eds) Magmatism in oceanic basins, vol. 42. Geological Society, London, Special Publications., pp. 313–345.

Workman RK, Hart SR (2005) Major and trace element composition of the depleted MORB mantle (DMM). Earth and Planetary Science Letters 231:53–72. https://doi.org/10.1016/j.epsl.2004.12.005.